Phase Fluctuation Chromatography of Diblock Copolymer of Poly(ethylene glycol) and Poly(L-lactide) for Fractionation by the Block Length Ratio

Dean Lee and Iwao Teraoka*

Herman F. Mark Polymer Research Institute, Polytechnic University, Six MetroTech Center, Brooklyn, New York 11201

Tomoko Fujiwara and Yoshiharu Kimura

Department of Polymer Science and Engineering, Kyoto Institute of Technology, Matsugasaki, Sakyo-ku, Kyoto, 606-8585, Japan

Received January 23, 2001; Revised Manuscript Received May 9, 2001

ABSTRACT: Phase fluctuation chromatography was used to separate a diblock copolymer PEG−PLLA by its block length ratio on a preparative scale, where PEG is poly(ethylene glycol) and PLLA is poly(L-lactide). A concentrated solution of the copolymer was injected into a column packed with surface-modified porous silica particles. Carboxymethyl-modified porous silica, in cooperation with size exclusion, separated the copolymer in a decreasing order of lactate content. To reverse the elution order, we grafted the surface of porous silica with PLLA chains by polymerizing L-lactide with surface silanol as initiator. A column packed with porous silica with long PLLA chains separated the copolymer in the opposite order against the size exclusion effect. Both separations resulted in fractionation primarily with respect to the length of PLLA block, indicating a broader length distribution of the PLLA block compared with the PEG block. The mass distribution of the separated fractions suggests a long tail at the high end of the PLLA block length. There was no evidence of correlation between the two block lengths.

Introduction

Chemical composition and its distribution (CCD) determine many properties of block copolymers in bulk,[1] suspensions,[2] and solutions.[3−5] The length distribution of each block and the ratio of the two block lengths are responsible for these properties. One example is a copolymer of a neutral block A with a short ionic block B in the bulk phase.[1] The copolymer forms microphase-separated spheres of block B in the continuous phase of block A. The sphere radius is determined by the longest block B in the copolymer sample. Another example is micelles formed by a PEG−PLLA diblock copolymer in water,[2] where PEG is poly(oxyethylene) and PLLA is poly(L-lactide). The block copolymer and its micelles have been investigated extensively for various applications.[6−10] The average of the micellar size, its distribution, and the shape of the micelle are affected by the overall molecular weight and the composition of the copolymer.[2] The critical micelle concentration of the solution, a measure for the stability of the micelles, increases with an increasing length of the PEG block relative to the PLLA block.[2]

The effects of the chemical composition and its distribution are usually studied by synthesizing block copolymers of different compositions. The chemical composition distribution can be artificially generated by mixing copolymers of known compositions, when they are monodisperse in composition.[1] The latter method is, however, limited to copolymers made by living polymerization. Block copolymers prepared in other methods including those used in industry have a broader CCD in general.

One of the open questions in the block copolymer synthesis is the correlation between the lengths of the two blocks. To answer this question, matrix-assisted laser desorption/ionization time-of-flight (MALDI/TOF) mass spectrometry was applied to characterization of the individual block length distribution in a block copolymer of polystyrene−poly(α-methylstyrene).[11,12] It was found that there is no correlation between the two blocks (random coupling). Although the full picture of CCD can be obtained by MALDI/TOF, the method can only be applied to copolymers with molecular weights up to 10 000 g/mol at best. The reliability of the data when applied to a polydisperse sample is questionable because of possible degradation and selective desorption.

HPLC allows us to separate a block copolymer with respect to the length of one block when operated at the critical condition of the other block.[13,14] Copolymer molecules with different lengths in the other block can be eluted at the same time by adjusting the pore size, mobile phase, and temperature. The enthalpy difference by the surface interaction between different lengths of the block is offset by the entropy difference of size exclusion at the critical condition.[15,16] The block, therefore, is masked from the recognition of the column. A PEG−PLLA diblock copolymer was separated by HPLC with respect to the number of lactate units at the critical condition of the PEG block.[17] The separated fractions were analyzed by MALDI/TOF. All the fractions presented the same molecular weight distribution of the PEG block within experimental errors, confirming the critical condition for PEG and the absence of correlation between the two blocks. HPLC is generally not suitable for high-molecular-weight samples, however, because use of the critical solvent condition for one of the blocks may lead to complete adsorption of the copolymer. Use of a stronger solvent to avoid the adsorption results in a loss of resolution.

Preparative separation of a diblock copolymer by the chemical composition is more difficult. The solvent−

10.1021/ma0101207 CCC: $20.00
Published on Web 06/07/2001

nonsolvent method, often used for preparative separation of a homopolymer by the molecular weight and a random copolymer by the chemical composition, does not work for the diblock copolymer. When a nonsolvent for one of the blocks is added to a solution of the diblock copolymer, microphase separation occurs to form micelles. They are suspended in the solution and do not precipitate for physical separation.

Phase fluctuation chromatography (PFC) was introduced several years ago to allow for preparative separation of a chemically heterogeneous polymer by the chemical composition.[18] PFC utilizes composition fluctuations in concentrated solutions of a copolymer. The column is packed with porous materials that have a surface modified to attract or repel one of the components of the copolymer. The concentrated solution is injected into the column until the first polymer is detected at the outlet. Then, the solvent is injected to displace the polymer in the column, and the eluent is collected into test tubes. In each plate of the column, different phases or domains of the heterogeneous solution are partitioned between the pore space and the interstitial volume of the porous packings according to the preference by the surface. Thus, the early eluent is enriched with copolymer components more strongly repelled by the surface.

In separation of a random copolymer of styrene and acrylonitrile (SAN) by PFC, it was found that a solvent that selectively dissolves the surface-repelled components produces a good separation.[18,19] The solution must be heterogeneous for a good separation, but not too much to cause precipitation or adsorption. The solution heterogeneity was evaluated in dynamic light scattering studies.[19,20] The pore size is also an important factor, since a small pore renders an often-unwanted strong size exclusion, and a large pore does not have sufficient surface moieties to interact with the copolymer.

Earlier, we applied PFC to separation of a mixture of PEG, PEG−PLLA, and PLLA−PEG−PLLA.[21,22] Among various surface moieties tested, a carboxymethyl (CML) surface exhibited the best separation when the solvent was dioxane, a good solvent for PLLA but a poor solvent for PEG. Helped by the size exclusion, components that are primarily triblock and therefore rich in lactate and of high molecular weight, eluted ahead of the other components. A high concentration (~25 wt %) of the injected solution was needed for the optimal separation, thus supporting the separation mechanism of PFC. Namely, spatial composition heterogeneity in the concentrated solution forces domains rich in surface-preferred components to occupy the stationary phase with an assistance of the high osmotic pressure. At lower concentrations, the solution is uniform, and each solute polymer chain interacts with the pore surface independently, resulting in a poorer resolution. In the study, we attempted to reverse the elution order by employing a surface friendly to PLLA, such as a diphenyl surface, a solvent friendly to PEG, such as dimethylformamide, and/or a larger pore size, but we failed to suppress the size exclusion to elute shorter chains earlier that consist mostly of PEG and PEG−PLLA.

The present study demonstrates that PFC can separate a diblock copolymer PEG−PLLA by the block length ratio in two opposite elution orders. To retain oxyethylene-rich components, we used the CML surface. To retain lactate-rich components, we grew PLLA on the surface of silica by polymerizing L-lactide with surface silanols as initiator and packed a column with the PLLA-modified porous silica. We could successfully retain lactate-rich components, in reversal to the separation by the CML surface. We evaluated the effects of the length of the grafted PLLA chains as well as the pore size on the resolution and preparative capacity of the separation. We also evaluated the stability of grafted PLLA.

Table 1. Characteristics of Controlled Pore Glasses

code	pore diam (Å)	particle size (mesh)	surf. area (m^2/g)	pore vol (mL/g)
CPG350B1	375	120/200	95	1.49
CPG350B2	343	120/200	67.5	0.97
CPG170B	182	120/200	112.7	0.97
CPG170B′	151	120/200	120.1	0.79
CPG75B′	82	120/200	224.5	0.37

Experimental Section

Materials. Controlled pore glasses (CPG) were obtained from CPG, Inc. The properties of the grades of CPG used in the present study, before surface modification, are listed in Table 1. The data were supplied by the manufacturer. The chemicals used for surface modification of CPG are as follows: L-lactide (LLA) and tin(II) 2-ethylhexanoate (2-Sn(Oct)$_2$) from Aldrich; silanization agents—diphenylmethylchlorosilane (DPMS), trimethylchlorosilane (TMS), and trimethylmethoxysilane (TMOS)—from Gelest. Solvents for various uses are as follows: 1,4-dioxane from Aldrich and Acros; *N*,*N*-dimethylformamide (DMF) and xylenes from Fisher; *p*-xylene from EM Science; $CDCl_3$ (99.8 and 100.0% deuterated) from Aldrich and Acros; CCl_4 from Aldrich. The chemicals used in the synthesis of the diblock copolymer include L-lactide (Purac Biochem, Netherlands), tin(II) 4-ethylhexanoate (4-Sn(Oct)$_2$) (Nacalai Tesque Co., Japan), and monomethoxy-terminated poly(ethylene glycol) (PEG5K) (Aldrich). PEG5K has a nominal molecular weight of 5000 g/mol.

N-[(Carboxymethyl)oxyacetyl]-3-aminopropylsilanetrioxy]-modified CPG was a gift from CPG, Inc. We call it CML*xxx*B, where *xxx* is the pore diameter in angstroms before the CPG was modified. Its properties are listed in Table 1 as CPG170B′ and CPG75B′.

Surface Modification of CPG by DPMS. Plain CPG (CPG350B1 and CPG170B) was soaked in concentrated HCl overnight at ambient and washed with deionized water several times until the pH of the supernatant was above 5. Then the CPG was dried in a convection oven followed by a vacuum oven at 60−80 °C. In the following, "drying" stands for this two-step process. A 20 wt % solution of DPMS in toluene was added in excess to the CPG. The reaction was maintained at 50−60 °C for 3 days while being stirred. Then toluene was used to remove unreacted DPMS. TMS (50 wt % in toluene) was added to end-cap the unreacted surface silanols at ambient with stirring overnight. Methanol was used to wash the CPG afterward. After drying, DPMS-treated CPG (DPM170B or DPM350B) was ready to pack a column.

Polymerization of L-Lactide onto CPG Surface. A 3.8 g sample of L-lactide was dissolved in 20 g of xylenes above 80 °C in nitrogen atmosphere. After adding 3.9 g of acid-washed and then dried CPG350B1, 0.25 g of 2-Sn(Oct)$_2$ was dropped in. The reaction mixture was heated to 120 °C and held at that temperature for 15 h with stirring under nitrogen flow. Afterward, the reaction mixture was cooled to 90 °C, and dioxane was added to remove free poly(L-lactide) (PLLA) that did not grow on the pore surface. When cooled to room temperature, the CPG was washed with acetone. We call this CPG PLLA350B1.

Polymerization of L-lactide onto two other grades of CPG (CPG350B2 and CPG170B) was slightly different. L-Lactide was recrystallized from distilled toluene, and the reaction was carried out in distilled *p*-xylene. A smaller amount of *p*-xylene (10 g) was used to increase the concentrations of the reactants. A 0.58 g sample of 2-Sn(Oct)$_2$ was added, and the temperature

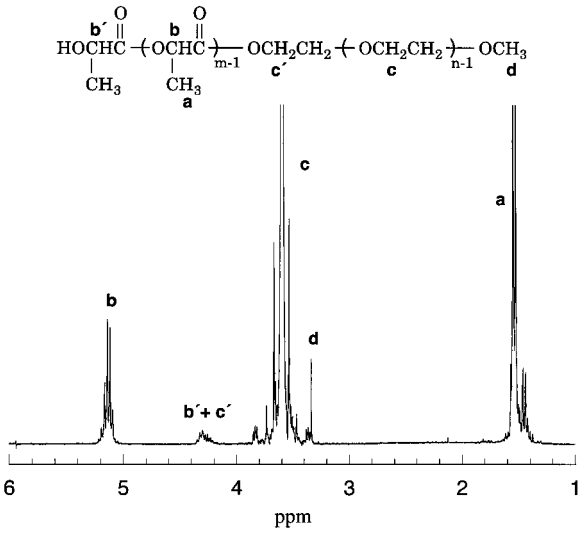

Figure 1. ^{1}H NMR spectrum of PEG5K−PLLA2K diblock copolymer with methoxy at the PEG terminal. The peaks are labeled with letters that represent the protons indicated in the figure.

was held at 135 °C. Other conditions were similar to those in the first polymerization of L-lactide. To end-cap the unreacted silanols, the washed and dried PLLA-modified CPG was soaked in TMOS for 72 h at ambient and washed with acetone. We call these CPGs PLLA350B2 and PLLA170B.

Surface Characterization. The surface modification was evaluated by using a Nicolet Avatar 360 FT-IR spectrometer. Surface-modified CPG was packed into a 1 mm path length IR-grade silica cell. CCl_4, nearly isorefractive with silica, was added into the cell to minimize the scattering of the IR beam. The cell was centrifuged to remove air bubbles and make the packing uniform. With silica present, the IR spectrum can be obtained only in the frequency range above 2200 cm^{-1}.

Synthesis of Diblock Copolymer. The synthesis protocol is the same as before.[23,24] L-Lactide was recrystallized from toluene. Monomethoxy-terminated PEG5K was lyophilized from benzene. 4-Sn(Oct)$_2$ was distilled under high vacuum. All the solvents were distilled before use. 4 g of L-lactide and 10 g of PEG5K were charged into a 300 mL flask. After the mixture was dried in a vacuum for 3 h, 0.73 mL of 4-Sn(Oct)$_2$ in toluene (10 mol % relative to PEG5K) was added to the mixture in a nitrogen atmosphere. The mixture was heated and stirred at 120 °C for 7 h. Then the product was cooled, dissolved in 100 mL of chloroform, and poured into a large excess of diethyl ether. The precipitate was filtered and vacuum-dried at 60 °C overnight to obtain the copolymer as powders in a 93% yield. Figure 1 shows its ^{1}H NMR spectrum (Bruker DPX-300) in $CDCl_3$; 1.56−1.6 (d, CH_3 for PLLA), 3.36 (s, OCH_3 for terminal methoxy), 3.6−3.7 (m, CH_2CH_2O for PEG), 4.3−4.4 (m, $COOCH_2$ connecting PEG with PLLA), and 5.1−5.2 (q, CH for PLLA). A singlet signal (d) due to the methoxy group and a multiplet signal (c′) of the $-COOCH_2-$ group at the joint suggest that a chain of PLLA has grown from the hydroxy tail of PEG. From the ^{1}H NMR spectrum (Bruker APX-500), the weight ratio of PLLA/PEG was calculated as 1.8/5, similar to L-lactide/PEG = 2/5 in the feed. The number-average molecular weight M_n of the block copolymer was estimated as 6800 g/mol from the NMR spectrum.

Figure 2 compares the retention curves of the copolymer PEG5K−PLLA2K and its precursor PEG5K obtained by size exclusion chromatography (SEC). The polydispersity (M_w/M_n; M_w is the weight-average molecular weight) is 1.19 and 1.06 for PEG5K−PLLA2K and PEG5K, respectively. The numbers are with respect to the polystyrene standards. Apparently attaching the PLLA block resulted in a broadening of the molecular weight distribution. Two polystyrene gel columns, Tosoh TSK gel G4000H8 and G2500H8, were used with chloroform as mobile phase (1 mL/min) at 35 °C.

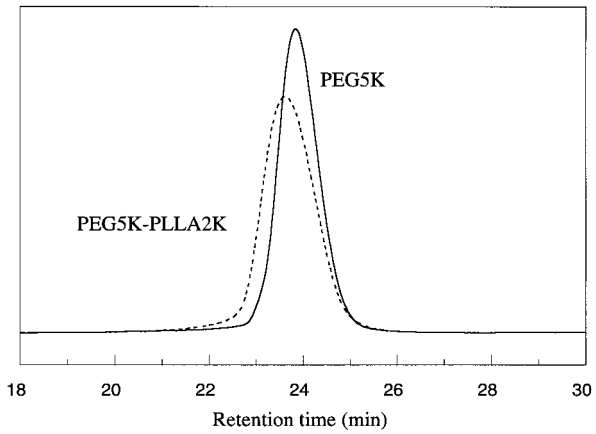

Figure 2. Normalized SEC chromatograms of PEG5K (solid line) and PEG5K−PLLA2K (dashed line).

Phase Fluctuation Chromatography. A stainless steel column (3.9 mm i.d. × 300 mm length) was packed with one of the modified CPGs. Before separation, the column was washed with the same solvent as the one used to dissolve the polymer. A 30 wt % solution of the polymer was prepared in dioxane at 65 °C. When the solution was cooled to room temperature, it became slightly hazy. The precipitate was observed when the temperature was below 20 °C. The solution was injected into the column at room temperature through a single-head HPLC pump (SSI, Acuflow II) at 0.2 mL/min (nominal). The eluent was dropped into ether to detect the polymer. When a precipitate was observed, the injection was switched from the solution to pure dioxane, and the eluent was led to a fraction collector (Eldex). At this moment, the polymer solution filled the whole column. In the separation with PLLA350B1, 20 drops were collected in fractions 1−12, 40 drops in fractions 13−14, 100 drops in fractions 15−16, and 300 drops in fractions 17−18. The other separations used a different protocol: 20 drops (1−10), 40 drops (11−12), 100 drops (13−14), and 300 drops (15−16). All the separations were conducted at room temperature. Dioxane and/or DMF was used to wash the column at 60 °C before the next batch of separation. The solutions in the test tubes were dried by blowing heated nitrogen and then in a vacuum oven at 60−80 °C overnight.

Composition Analysis. The composition of the copolymer in each fraction was analyzed by using a Bruker DPX-300 NMR spectrometer in $CDCl_3$ with MacNuts software. Integrals in 5.4−5.0 ppm ($I_{5.2}$, methine of lactate), in 3.2−4.0 ppm ($I_{3.6}$, methylene of oxyethylene), and at around 3.36 ppm ($I_{3.36}$, methoxy at PEG terminal) were used to estimate the chemical composition. The average mole fraction of LLA (x_{LLA}) in each fraction was calculated as

$$x_{LLA} = \frac{I_{5.2}}{I_{5.2} + I_{3.6}/4}$$

Here we neglect the contribution of the terminal methoxy peak to $I_{3.6}$.

To estimate the number-average block lengths of PEG (N_{PEG}) and of PLLA (N_{PLLA}), we consider that $I_{5.2}$ does not include terminal methine of PLLA and $I_{3.6}$ does not include PEG methylene at the joint with the PLLA block but includes the terminal methoxy. Comparison of $I_{3.36}$, $I_{3.6}$, and $I_{5.2}$ yields N_{PEG} and N_{PLLA} as

$$N_{PEG} = \frac{1}{4}\left(\frac{I_{3.6}}{I_{3.36}} \times 3 - 1\right)$$

$$N_{PLLA} = \frac{I_{5.2}}{I_{3.36}} \times 3 + 1$$

Unlike the analysis by the 500 MHz spectrometer (APX-500), the routine analysis by the 300 MHz spectrometer did not

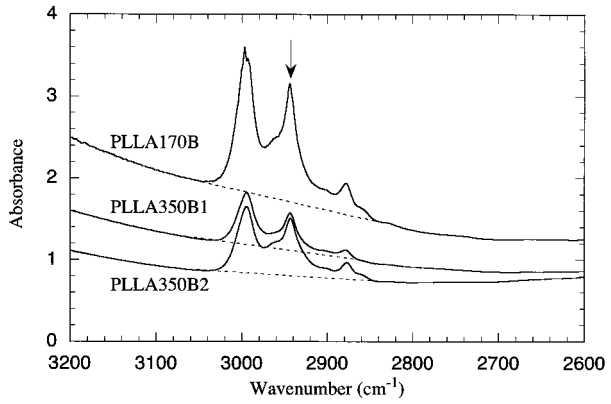

Figure 3. IR absorbance spectra of CPGs grafted with PLLA before end-capping. The peak absorbance above the baseline (dashed line) at the wavenumber indicated by the arrow was used to calculate the grafting density.

resolve the methoxy peak sufficiently well from the nearby methylene peak. The results of N_{PEG} and N_{PLLA} are slightly overestimated.

The errors in the estimates of x_{LLA}, N_{PEG}, and N_{PLLA} are 3%, 4%, and 6%, respectively, at the worst when the concentration was low in late fractions. For most of the fractions, the errors, especially the error of x_{LLA}, are much smaller.

Results and Discussion

Evaluation of Surface Modifications. Figure 3 shows the IR spectra of PLLA170B, PLLA350B1, and PLLA350B2 immersed in CCl_4 before end-capping. Air was used as background. The peaks at 2997 and 2944 cm^{-1}, also observed in the solution of free PLLA, are ascribed to the surface PLLA. IR spectra were also obtained for surface-modified DPM170B and DPM350B immersed in CCl_4 after end-capping (not shown). The absorption peaks ascribed to phenylene C−H stretching were observed at 3072, 3053, and 3025 cm^{-1}. Another peak at 2962 cm^{-1} was due to methyl C−H stretching of both DPMS and TMS end-capping. Using the absorbance data, we estimated the grafting density of DPMS and PLLA on the pore surface as follows.

We first obtained the calibration curve that relates the absorbance and the concentration of DPMS. The IR spectra were measured for solutions of free DPMS in CCl_4 at four different concentrations up to 0.189 mol/L. The plot of the absorbance A_{3072} at 3072 cm^{-1} as a function of molar concentration M of DPMS was on a straight line through the origin: $A_{3072} = 8.90 \times M$ (mol/L). We obtained the calibration curve also for free PLLA. We used $CDCl_3$ (100.0% deuterated) as the solvent because PLLA did not dissolve in CCl_4. The IR absorbance spectra were measured at seven different concentrations up to 0.317 mol/L (concentration of L-lactate monomer). The absorbance at 2945 cm^{-1} (the peak position was slightly shifted from that of attached PLLA) vs concentration was on a straight line through the origin: $A_{2945} = 1.76 \times M$ (mol/L). Separately we confirmed that A_{2944} of the end-capped, PLLA-modified CPG was the same between the two immersing liquids, $CDCl_3$ and CCl_4.

Comparison of the absorbance for a given surface-modified CPG sample with the relevant calibration curve yields the molar concentration M of DPMS anchored to the pore surface or the monomer molar concentration of PLLA on the surface. The results are listed in Table 2. Separately, we estimated the packing density D of the CPG particles from the mass and volume of the packed bed of CPG in the IR cell. Finally, the surface molar densities of DPMS and PLLA were calculated by using the following formula and are listed in Table 2.

Table 2. Evaluation of Surface Modifications

code	M (mol/L)	D (g/mL)	molar density (mol/m^2)	loading (g/g CPG)	DP
PLLA350B1	0.264	0.299	9.29×10^{-6}	0.064	4.7
PLLA350B2	0.391	0.404	1.44×10^{-5}	0.070	14
PLLA170B	0.807	0.356	2.01×10^{-5}	0.163	19
DPM350B1	0.0560	0.299	1.97×10^{-6}	0.040	
DPM170B	0.0415	0.356	1.03×10^{-6}	0.025	

$$\text{surface molar density (mol/m}^2) = \frac{M \text{ (mol/L)}/1000}{D \text{ (g/mL)} \times \text{surface area (m}^2\text{/g)}}$$

The total loading of DPMS or PLLA per unit mass of parent CPG is also listed.

The two surface molar densities of DPMS in the table are equivalent to 0.012 and 0.0062 functional groups per Å^2 in DPM350B1 and DPM170B, respectively. These numbers are comparable to those reported earlier.[25] Using the estimate of 0.05 per Å^2 for the number of surface hydroxyl groups on a fully hydroxylated surface,[26] we find the degree of substitution of surface silanol by DPMS in CPG350B1 and CPG170B was ca. 25% and 12%, respectively.

Assuming that PLLA and DPMS have the same grafting density on the surface of a given CPG, the degree of polymerization (DP) of PLLA was estimated by dividing the surface molar density of PLLA by that of DPMS on the same CPG. The results are listed in Table 2. We could not follow this method for PLLA350B2, because we did not prepare DPMS-substituted CPG from the same parent CPG. To estimate DP of PLLA in PLLA350B2, we use the grafting density of DPMS on the surface of CPG170B based on the assumption that the grafting density depends on the pore volume. Comparison of the separation performance of PLLA350B2 with those of other PLLA-modified CPGs to be shown later indicates that our assumption is not off the point. Thus, we prepared three grades of PLLA-grafted CPG: PLLA350B1 with a large pore, short PLLA; PLLA350B2 with a large pore, long PLLA; and PLLA170B with a small pore, long PLLA.

When fully extended, the grafted PLLA chains have an approximate length of 17, 52, and 70 Å in PLLA350B1, PLLA350B2, and PLLA170B, respectively (monomer unit length = 3.68 Å). The monomer volume of a lactate unit, a half of the volume of lactide calculated by ChemSketch (Advance Chemistry Development), is 101 Å^3. The surface area of PLLA per repeating unit is thus 27.4 Å^2. Each grafted chain has an effective surface area of 27.4 Å^2 × DP. In PLLA170B, for instance, the surface area per grafted chain is 521 Å^2. Therefore, grafting a polymer chain onto the surface is an efficient way to increase the interaction of the stationary phase with substrates. The surface area will shrink, however, when a nonwetting mobile phase enters the pore.

To have a better idea about the volume of the PLLA chains in the pore, let us consider a 10 Å section of a cylindrical pore of diameter 182 Å (CPG170B). The surface area of this ring section is $10 \times 182 \times \pi = 5.7 \times 10^3$ Å^2. Then $5.7 \times 10^3 \times 0.0062 = 35$ is the estimated

Table 3. Recovery of Injected Polymer

	mass of solution injected (g)	recovery (%)	$\langle N_{PLLA}\rangle$	$\langle N_{PEG}\rangle$	$\langle x_{LLA}\rangle$	$\langle \Delta x_{LLA}^2\rangle^{1/2}$
original			28.9	142	0.164	
(error)			1.2	4	0.002	
CML75B	2.49	100.6	30.1	148	0.162	0.0319
CML170B	2.78	100.7	28.5	141	0.163	0.00963
PLLA170B	1.92	96.0	29.0	143	0.164	0.0272
PLLA350B1	3.29	98.7	29.4	143	0.166	0.00766
PLLA350B2	2.63	98.2	29.9	144	0.167	0.0231
DPM170B	2.66	96.7	29.9	146	0.165	0.00399
DPM350B1	3.28	98.4	28.8	142	0.164	0.00470

number of the grafted chains on the ring. These chains combined occupy a volume of 101 × 19 × 35 Å^3 = 67 nm^3. It is about 26% of the pore volume of the ring section. Since dioxane swells PLLA chains, we expect that the pore volume available for the copolymer solution is smaller than 0.97 mL/g × 74% = 0.72 mL/g.

Recovery of Injected Polymer. Table 3 lists the mass of the injected block copolymer solution and some analysis results related to the recovery of the injected polymer in each batch of separation. The mass of the injected solution is a measure of the actual pore volume of the column and is affected by the surface interaction and the size exclusion. Compared for the same surface chemistry, the injected amount is smaller when the CPG has a smaller pore volume, a reasonable result. Made from the same parent CPG, DPM170B has a greater injection amount than PLLA170B does. Despite a smaller pore volume in the parent CPG, CML170B has a larger injection amount compared with DPM170B. From these two comparisons, we can arrange the three surfaces in the decreasing order of the injection amount in case they are prepared from the same parent CPG: CML170B > DPM170B > PLLA170B. The second inequality is reasonable, as long PLLA chains grafted on the pore surface decreases the pore volume. In contrast, PLLA350B1 that has shorter PLLA chains has almost the same injection amount as DPM350B does. Overall, the large injection amount with the CML surface is noteworthy, especially for CML75B which has a small pore volume in the parent CPG. As we will see below, this surface attracts PEG blocks, the main part of the diblock copolymer. The easy accommodation of the copolymer by the CML surface has resulted in a larger injection amount before the first polymer comes out of the column. From the injection amounts alone, we can expect that PLLA surface dislikes PEG blocks, as we intended.

The mass percentage of the recovery is calculated as the ratio of the total mass of copolymer in the fractions collected to the mass of copolymer in the injected solution. It provides the information about possible adsorption of the diblock copolymer onto the pore surface as well as possible degradation of the copolymer and grafted PLLA. The recovery was nearly 100% for all separations.

The $\langle N_{PLLA}\rangle$, $\langle N_{PEG}\rangle$, and $\langle x_{LLA}\rangle$ are the averages of N_{PLLA}, N_{PEG}, and x_{LLA}, respectively, for all the fractions collected in the separation, weighted by the mass of the copolymer in each fraction. The table lists also the averages for the original diblock copolymer before separation and the errors in the estimation. The errors are the standard deviation in three measurements. The values of $\langle N_{PLLA}\rangle$, $\langle N_{PEG}\rangle$, and $\langle x_{LLA}\rangle$ are all equal to those of the original copolymer within experimental errors, indicating that adsorption of specific components of the copolymer is negligible. The $\langle \Delta x_{LLA}^2\rangle^{1/2}$ is the root-mean-square of $x_{LLA} - \langle x_{LLA}\rangle$ for all the fractions weighted by the mass of the polymer. A separation that produces fractions in a broader span in x_{LLA} has a greater $\langle \Delta x_{LLA}^2\rangle^{1/2}$.

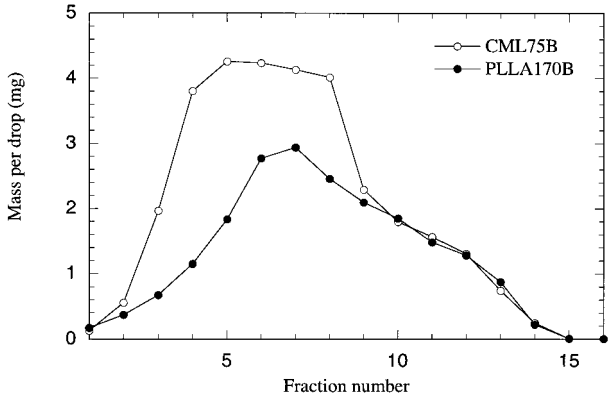

Figure 4. Mass of polymer contained in a drop of the eluent in the separation by CML75B (open circles) and PLLA170B (closed circles).

The values of $\langle N_{PLLA}\rangle$ and $\langle N_{PEG}\rangle$ listed in the table lead to the number-average block molecular weights of 2100 and 6200 g/mol for the PLLA and PEG blocks, respectively. These values are slightly larger than those estimated from the 500 MHz NMR spectrum.

Concentration of the Eluent. Figure 4 compares the concentration of the eluent in the separations with the PLLA170B and CML75B. The average mass of the polymer per drop of the eluent in each fraction is plotted as a function of the fraction number. In both separations, the concentration maximized in the middle fractions. In the separation with CML75B, fractions 4−8 were more concentrated than the injected solution (30 wt %), with the highest at 36 wt %. In PFC, the concentration increase can occur, when the polymer, being left behind in the pore from the front end of the transported solution, was released into already concentrated later eluent. In the separation with PLLA170B, the peak concentration (25 wt %) was lower, and the plateau was narrower. The pattern of the concentration change in other separations was somewhere between these two curves.

Because the loading amount in the separation with PLLA170B was smaller than that with CML75B, the concentration of eluent in the PLLA170B separation should be lower as the same volume of eluent was collected in each fraction. The lower concentration was manifested in the early fractions but not in the late fractions. The skewness of the curve will be discussed with the mass fraction plots shown later.

Opposite Separation Trends. Figure 5 compares the results of separation with CML75B and PLLA170B. The plots of x_{LLA} and the mass fraction of the copolymer (the ratio of the mass in each fraction to the total mass of the fractions) are shown as a function of the fraction number in part a of Figure 5. The mass fraction plot is not the same as the concentration plot in Figure 4, because the number of drops collected in each fraction was different. The gray bar depicts x_{LLA} of the original copolymer. With CML75B, x_{LLA} decreased with an increasing fraction number except for the last two fractions that had only a small mass. The overall trend of x_{LLA} was reversed in the separation with PLLA170B, although x_{LLA} decreased in early fractions (1−5). In both

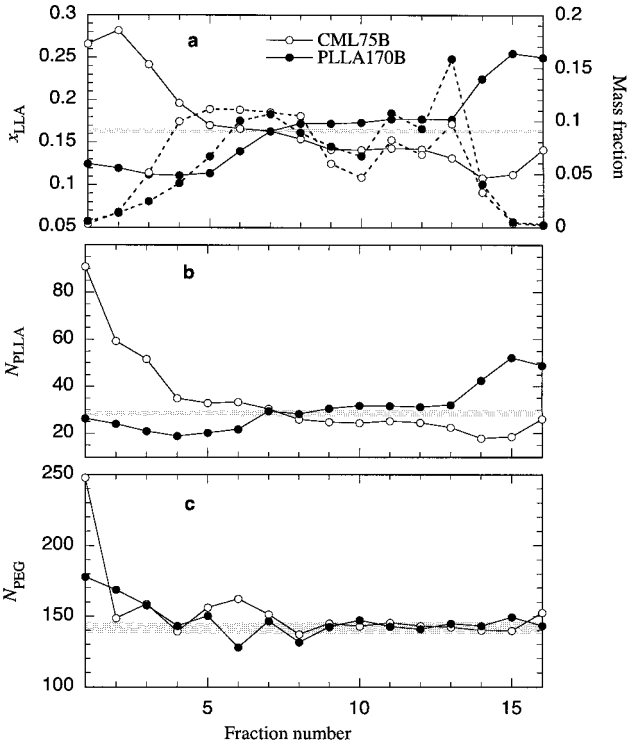

Figure 5. Comparison of the separations by CML75B (open circles) and PLLA170B (closed circles). (a) The x_{LLA} (solid line) and mass fraction (dashed line), (b) N_{PLLA}, and (c) N_{PEG} are plotted as a function of the fraction number. The gray rectangles represent the original copolymer.

separations, x_{LLA} reached a plateau consisting of fractions 9−12 after passing the x_{LLA} value of the original sample. The mass percentage plot of the CML75B separation indicates a larger amount of polymer in early fractions. In the PLLA170B separation, late fractions had a higher relative mass. Both correspond to a high x_{LLA}.

Parts b and c of Figure 5 show the lengths of the PLLA and PEG blocks, respectively, in each fraction. The N_{PLLA} plots follow closely the corresponding x_{LLA} plots. There is a wide variation in N_{PLLA} from fraction to fraction. In contrast, N_{PEG} is almost the same in all fractions as that of the original copolymer, although there is a downward trend in the early fractions (1−4) in the PLLA170B separation and N_{PEG} of fraction 1 is large in the CML75B separation.

The opposite trend between the two separations is due to the different properties of the surfaces. The CML surface has favorable interactions with PEG blocks and/or adverse interactions with PLLA blocks. It tends to retain copolymers with higher oxyethylene contents. PEG is known to form a complex with poly(acrylic acid) or poly(methacrylic acid).[27,28] This is why the injection amount was unusually large in the separation with the CML surface. In contrast, the PLLA surface tends to retain copolymers with higher lactate contents. The decrease of x_{LLA} and N_{PLLA} in the early fractions of the PLLA170B separation is ascribed to the size exclusion effect. Initially segregated to the mobile phase by the surface interaction at high concentrations, the low-x_{LLA} components were then separated among themselves by the size. As the solution containing those components was transported along the column, the concentration dropped. A concomitant decrease in the compositional fluctuation made the size exclusion effect overwhelm the

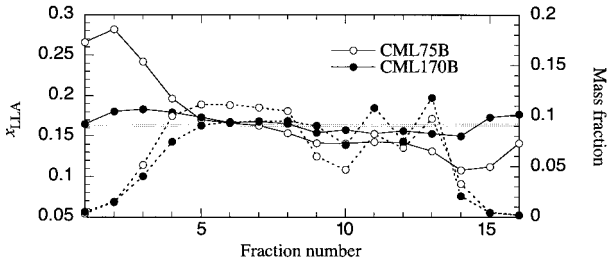

Figure 6. Comparison of the separations by CML75B (open circles) and CML170B (closed circles). The x_{LLA} (solid line) and mass fraction (dashed line) are plotted as a function of the fraction number.

surface interaction in the front portion of the eluent. The CML75B separation also exhibited the size exclusion effect, but it was synergetic with the surface interaction. Both the surface interaction and size exclusion cooperated to exclude the high-x_{LLA} components. This synergy explains why the CML75B separation had the best resolution among all the separations, as manifested in the greatest $\langle \Delta x_{LLA}^2 \rangle^{1/2}$ in Table 3.

The plateau region in fractions 9−12 was due to the overloading of the column. CML75B secured a relatively large amount of high-x_{LLA} components in the early fractions, depleting these components from the copolymer that had been partitioned to the stationary phase and eluted later. Therefore, the plateau in CML75B has a lower x_{LLA} than the original copolymer does. The same applies to PLLA170B.

The similarity in the shape between the curvesof N_{PLLA} and x_{LLA} indicates that the composition distribution was governed by the length distribution of the PLLA block. In contrast to the broad distribution in N_{PLLA}, the PEG block has a much narrower distribution. This result agrees with the broadening in the SEC chromatogram when the PLLA block was added.

In the PLLA170B separation, the surface interaction cooperated with the size exclusion effect to repel longer PEG blocks, despite the narrow distribution of the PEG block length. In the early fractions (1−4), N_{PEG} decreased gradually before it reached the value of the original copolymer. In contrast, the surface interaction worked against the size exclusion for the PEG block in the CML75B separation, resulting in a poor separation with respect to N_{PEG}.

In another study, we separated the homopolymer PEG5K using CML75B. The plot of N_{PEG} was similar to the one shown in Figure 5c. The extremely high N_{PEG} ($\cong$ 248) was also observed (data not shown). It indicates presence of a small amount of high-molecular-weight components that cannot enter the small pore despite preferable interaction. A closer look at the SEC chromatogram of PEG5K shows a small leading edge to the left of the main peak (Figure 2). The low value of x_{LLA} in fraction 1 is due to the high N_{PEG}.

As seen in the above discussion, the resolution of PFC was compromised by the distribution of the two block lengths. For more detailed analysis of PFC, we need a copolymer sample with a narrower distribution in either block.

Effect of Pore Size: CML Surface. Figure 6 compares the separation performance by the two pore sizes of the CML surface. The plots of x_{LLA} and the mass fraction are shown. Overall, x_{LLA} decreased with an increasing fraction number, but the span in x_{LLA} in the separated fractions was narrower in the separation with

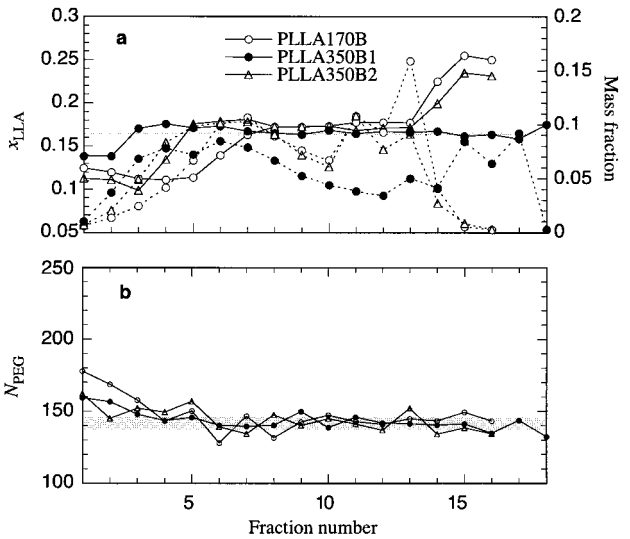

Figure 7. Comparison of the separations by PLLA170B (open circles), PLLA350B1 (closed circles), and PLLA350B2 (triangles). (a) The x_{LLA} (solid line) and mass fraction (dashed line) and (b) N_{PEG} are plotted as a function of the fraction number.

CML170B compared with CML75B. The relative mass of the copolymer with a high x_{LLA} was smaller compared with that of CML75B.

The plot of N_{PLLA}(not shown) is again similar to the plot of x_{LLA} for the separation with CML170B. The N_{PLLA} decreased from 35.0 in fraction 1 to 25.4 in fraction 13 and bounced back to 32.3 in the last fractions. The fraction 1 of the CML170B separation had $N_{PEG} = 172$. The other fractions had N_{PEG} almost identical to that of the original copolymer (not shown).

Use of CML-modified CPG with a larger pore size decreased both the size exclusion effect and the surface interaction. Note that a porous material with a greater pore size has a smaller surface area (Table 1). Because both effects cooperated in separating the copolymer by x_{LLA} in the CML separation, the reduction of the two effects resulted in a much poorer separation.

In fractions 15 and 16 of the CML separation, the NMR spectra had a peak at 5.05 ppm ascribed to the methine proton next to COOH (i.e., *H* in HOOCC*H*(CH_3)-CO−). The integral of this peak is 20% (fraction 15) and 18% (fraction 16) of $I_{5.2}$ (main methine peak) in the CML75B separation; it is 15% (fraction 15) and 12% (fraction 16) of $I_{5.2}$ in the CML170B separation. We consider that the carboxyl group of the CML surface catalyzed the decomposition of PLLA blocks, resulting in free PLLA. The copolymer that stays longer in the stationary phase will be more vulnerable. The decomposed PLLA will stay longer in the stationary phase and come out in the last fractions, resulting in the high x_{LLA}. Nonetheless, the decomposition did not affect the separation significantly because the mass fraction is small in the last two fractions.

Effect of Pore Size and DP of Grafted PLLA. Figure 7a compares x_{LLA} and the mass fraction in the separations with PLLA170B (DP = 19), PLLA350B1 (DP = 4.7), and PLLA350B2 (DP = 14). In the PLLA350B1 separation, x_{LLA} was lower than that of the original only for the first two fractions. In the PLLA350B2 separation, x_{LLA} was lower in the first three fractions compared with the same fractions in the PLLA170B separation. Then x_{LLA} increased to reach a plateau in fraction 5. The x_{LLA} in fractions 5−13 was slightly greater than that of the original copolymer. Compared with PLLA170B, the PLLA350B2 separation reached the plateau in an earlier fraction and has a lower x_{LLA} in the late fractions (11−16).

The mass fraction plots indicate that the relative mass in the early fractions is in the order of PLLA350B1 > PLLA350B2 > PLLA170B. We cannot compare the mass fraction in later fractions, because the collection protocol in PLLA350B1 was different from the one used in the other two separations.

The plots of N_{PLLA} (not shown) were similar to those of x_{LLA}. In the separation with PLLA350B1, the first two fractions had N_{PLLA} (26.7 and 26.0) lower than that of the original copolymer; all the other fractions had values slightly higher than (or nearly equal to) that of the original sample. In the separation with PLLA350B2, N_{PLLA} was 21.6, 19.1, and 17.6 in the first three fractions, lower compared with the same fractions in the PLLA170B separation. Then N_{PLLA} increased and reached a plateau at fraction 5. The last two fractions had $N_{PLLA} = 43.4$ and 41.4, lower than that of the same fractions in the PLLA170B separation.

In Figure 7b, N_{PEG} in the PLLA350B1 separation decreased in the first four fractions, but it was smaller compared with that in PLLA170B. In the PLLA350B2 separation, it was fraction 1 and fractions 3−5 that had a greater N_{PEG} than that of the original copolymer.

PLLA350B1 and PLLA350B2 have a smaller surface area to interact with the polymer and a weaker size exclusion effect compared with that of PLLA170B. Although the pore size was similar, the performance difference between PLLA350B1 and PLLA350B2 is remarkable. The long PLLA chains and hence the high lactate density were essential in partitioning lactate-rich components into the stationary phase. The large pore size and the high DP of surface PLLA gave PLLA350B2 probably the highest ratio of the surface interaction to the size exclusion effect for dilute solutions, as achieved in the lowest x_{LLA} and N_{PLLA} in the early fractions.

Correlation of N_{PLLA} and N_{PEG}. We prepared a plot of N_{PEG} vs N_{PLLA} for all the separations (not shown). A slightly positive correlation was observed in the early fractions for the separations by CML75B and PLLA170B. It is probably due to the size exclusion effect, which artificially partitions components with long PLLA and PEG blocks to the mobile phase. In the PLLA350B2 separation, the relatively high surface interaction destroyed the correlation in the early fractions as indicated by the absence of a decreasing trend of N_{PEG}. The absence of correlation in this separation suggests that the correlation observed in the other separations is due to the size exclusion.

If the diblock copolymer had a negative correlation between N_{PEG} and N_{PLLA} (a longer PLLA tends to grow on a shorter PEG; a shorter PLLA tends to grow on a longer PEG), our PFC would have separated them handily. The job is easier than to separate the diblock copolymer by the chemical composition that has no correlation or a positive correlation between the two lengths. CML75B, for instance, would have yielded early fractions with large N_{PLLA} and small N_{PEG}. From these facts, we consider it likely that N_{PLLA} and N_{PEG} are not correlated, in agreement with previous studies.[17]

Separation by Diphenyl Surface. We also performed separation by the diphenyl (DPM) surface using DPM170B and DPM350B1. In the plots of x_{LLA}, N_{PLLA}, and N_{PEG} (not shown), almost all the data are close to

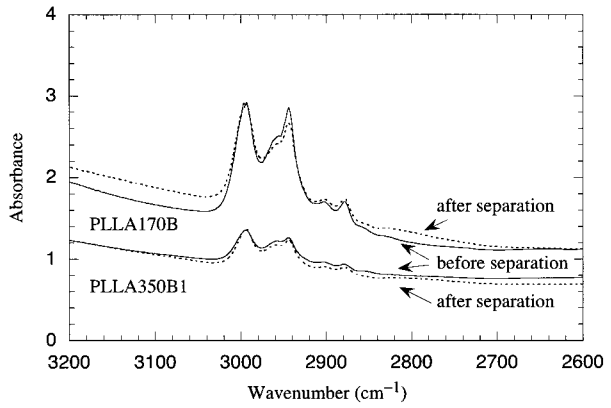

Figure 8. IR absorbance spectra of end-capped PLLA170B and PLLA350B1 before use (solid lines) and after four batches of separation (dashed lines).

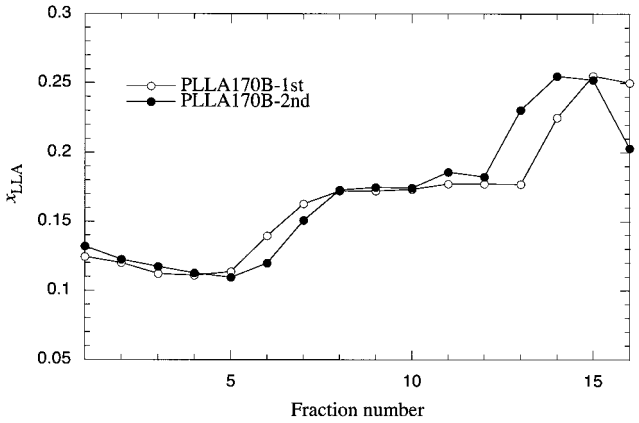

Figure 9. Comparison of the separation results for the first (open circles) and fourth (closed circles) uses of the same column PLLA170B. The x_{LLA} is plotted as a function of the fraction number.

those of the original copolymer, indicating a weak resolution by the DPM surface. The latter is also evident in the small $\langle \Delta x_{LLA}^2 \rangle^{1/2}$ (Table 3). Apparently, the DPM surface has weaker interactions with the copolymer than the other two surfaces do. The size exclusion effect was also less significant in DPM170B and DPM350B1 compared with the other columns of the same pore size. This result suggests that the attractive interaction between the surface and the PLLA block compensates the size exclusion effect to the extent to cancel the molecular weight dependence of the two effects. The situation resembles HPLC at the critical condition of adsorption.[15,16]

PLLA Block in the Copolymer. The mass fraction plots of Figure 5a indicate that a high x_{LLA} corresponds to a large relative mass in the two separations. As shown in the other mass fraction plots and concentration plots as well, it was easier to secure a large amount in the high end of the distribution of N_{PLLA}. This result suggests a tail extended toward a high N_{PLLA} in its distribution, in agreement with the results obtained for other PEG−PLLA copolymers[17] and other diblock copolymers.[11,12]

Degradation of Grafted PLLA. It is well-known that the silyl ester linkage (Si−O−CO−R), which anchors the PLLA chains onto the silica surface, is sensitive to water for hydrolysis.[29] Therefore, we tested possible degradation of grafted PLLA chains. After four batches of separation by each of the columns packed with PLLA350B1 and PLLA170B, a small amount of PLLA−grafted CPG was removed from the column to measure the IR spectra (Figure 8). The peak area in 3056−2858 cm^{-1} decreased by 5.2% in the PLLA350B1 column and 18.6% in the PLLA170B column. The decrease implies degradation of attached PLLA chains. We suspect that peroxides produced by dioxane were responsible for the decomposition. We believe that the degradation occurred mostly when the column was washed in dioxane at 60 °C after each separation but not during the separation at room temperature because (1) recovery of the copolymer was less than 100% (Table 3), with no extra polymer released from the pore surface; (2) almost all the averages of x_{LLA}, N_{PLLA}, and N_{PEG} are equal to those of the original sample within experimental errors; and (3) the peak at 5.05 ppm in the NMR spectra, which corresponds to the decomposed homopolymer PLLA, was insignificant and much smaller than the corresponding peaks observed in the late fractions with the separation by the CML surfaces. It has turned out that our silyl ester linkage was unusually stable in the two columns. We speculate that the hydrophobic environment of the stationary phase, created by the grafted PLLA and end-capping trimethylsilyl, prevents polar molecules such as water from accessing the anchoring point. The degradation of the grafted PLLA did not affect the separation performance, as seen below.

Reproducibility. Figure 9 compares x_{LLA} for the first use (PLLA170B-1st) and fourth use (PLLA170B-2nd; 2nd separation of the diblock copolymer) of the same PLLA170B column. The PLLA170B-2nd had a lower x_{LLA} in fractions 5−7 and a higher x_{LLA} in fraction 13 compared with those of PLLA170B-1st. Otherwise, the two plots are close to each other with a similar shape. Overall, PLLA170B-2nd showed a slightly better separation compared with PLLA170B-1st, although the purity was slightly poorer in fractions 1−4. The comparison demonstrates that the degradation of the surface PLLA did not deteriorate the separation. We rather see an improvement in the overall separation, as fewer fractions have x_{LLA} close to that of the original copolymer. The higher, more uniform packing density of CPG particles after a few runs may be responsible for the improvement. We also did the separation with CML75B, PLLA350B1, and PLLA350B2 columns twice. The results were reproducible.

Evaluation of Preparative Separation. To evaluate the preparative capability of each separation, we first sorted all the fractions obtained in the separation in the increasing order of x_{LLA}. Then we prepared a plot of x_{LLA} as a function of the cumulative mass fraction. The result is a step function that consists of as many horizontal sections as the total number of fractions. An additional point, lower or higher by a half step than the first or last fraction, was added at each end. An example of such plots is shown in the inset of Figure 10. We drew a smooth curve that passes between the dots on the step function, in hopes that the curve would represent the step function as if the eluent were collected in infinite number of fractions. The curves thus obtained are shown in Figure 10 for PLLA170B, CML75B, and DPM170B.

A better separation has a curve that deviates further from the horizontal. It is evident in this figure that CML75B gave the optimal separation, followed by PLLA170B, in agreement with other presentations of the separation results. The poor separation by DPM170B

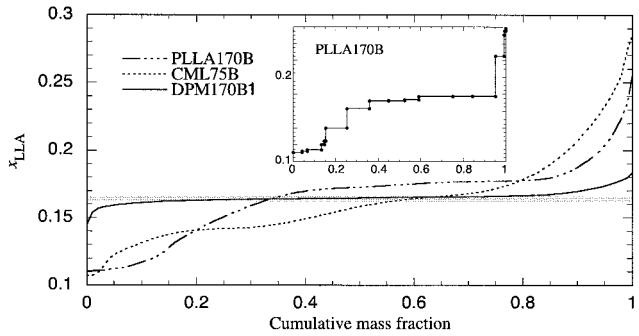

Figure 10. Evaluation of the preparative performance of the PLLA170B (dash−dotted line), CML75B (dashed line), and DPM170B (solid line) separations. The x_{LLA} is plotted as a step function of the cumulative mass fraction (shown in the inset for PLLA170B) and then fitted by a smooth curve. The curves are shown for comparison.

is also evident in the figure, as the curve is almost horizontal at x_{LLA} of the original copolymer, except for the left and right ends.

The plot can be used to estimate what percentage of the original copolymer would be secured in a fraction with x_{LLA} above or below a given value. Suppose that we want to collect a fraction with x_{LLA} lower than 0.12 or higher than 0.20, i.e., 0.04 lower or higher than 0.16 $= x_{LLA}$ of the original copolymer. Then PLLA170B can collect 12% of the original sample in the fraction with x_{LLA} lower than 0.12 and 5% in the fraction with x_{LLA} higher than 0.20. CML75B can collect 5% and 10% in the two fractions, respectively. It shows that PLLA170B is good at collecting the fraction with low-x_{LLA} and CML75B is good at high-x_{LLA} portion of the copolymer. This result agrees with the separation mechanism of PFC. It excels in the early fractions. This is why we need two surfaces that exhibit the opposite trend.

Conclusion

We demonstrated that use of CPG with surface-grafted PLLA reverses the elution order of the PEG−PLLA diblock compared with the carboxymethyl-modified CPG. PLLA grafted on the CPG surface efficiently increased the surface interaction. It cooperated with a high concentration of the injected solution to enhance the surface interaction in PFC. The enhanced surface interaction overcame the size exclusion effect to retain components with a high x_{LLA}, resulting in a separation as good as the separation with the CML surface. In the latter separation, the surface interaction cooperated with the size exclusion effect to retain low-x_{LLA} components. The PLLA surface has another advantage: Unlike the CML surface, it does not decompose the copolymer.

In successful PFC, early fractions and late fractions have a chemical composition distinctly different from that of the original sample. The early fractions are more easily collected compared with the late fractions because of a higher concentration. In contrast, late fractions stay longer in the column and therefore are more vulnerable to contamination or decomposition. The opposite separation trends as we found in the PLLA and CML surfaces allow us to obtain fractions in the two ends of the composition distribution efficiently.

Although PFC was developed primarily for preparative purposes, the enhanced surface interaction demonstrated in the present study will allow us to seek its analytical capability. PFC has several advantages compared with typical analytical separation methods such as HPLC at the critical condition: (1) the method development is easier; (2) PFC is not as vulnerable to a slight change in the separation condition such as the mobile phase composition and the temperature; (3) PFC can be applied to a broader range of molecular weight. We are currently testing the analytical capability of PFC for a mixture of tri- and diblock copolymer and other copolymer systems.

We note that PFC does not have a firm support by thermodynamic studies at this moment. There has been no study, either theoretical, experimental, or by simulation, on the partitioning of a random copolymer or a block copolymer with a modified surface in the semidilute solution. Coexistence of different types of interaction, between the surface and each copolymer component, between different components, and between solvent and each component, complicates the partitioning.

Acknowledgment. We appreciate financial support from NSF-DMR 9975650.

References and Notes

(1) Nguyen, D.; Zhong, X.-F.; Williams, C. E.; Eisenberg, A. *Macromolecules* **1994,** *27*, 5173.
(2) Nagasaki, Y.; Okada, T.; Scholz, C.; Iijima, M.; Kato, M.; Kataoka, K. *Macromolecules* **1998**, *31*, 1473.
(3) Jian, T.; Anastasiadis, S. H.; Semenov, A. N.; Fytas, G.; Adachi, K.; Kotaka, T. *Macromolecules* **1994**, *27*, 4762.
(4) Pan, C.; Maurer, W.; Liu, Z.; Lodge, T. P.; Stepanek, P.; von Meerwall, E. D.; Watanabe, H. *Macromolecules* **1995**, *28*, 1643.
(5) Semenov, A. N.; Anastasiadis, S. H.; Boudenne, N.; Fytas, G.; Xenidou, M.; Hadjichristidis, N. *Macromolecules* **1997**, *30*, 6280.
(6) Kimura, Y.; Matsuzaki, Y.; Yamane, H.; Kitao, T. *Polymer* **1989**, *30*, 1342.
(7) Cohn, D.; Younes, H. *J. Biomed. Mater. Res.* **1988**, *22*, 993.
(8) Zhu, K. J.; Song, B.; Yang, S. *J. Polym. Sci., Polym. Chem. Ed.* **1989**, *27*, 2151.
(9) Gref, R.; Mibamitake, Y.; Peracchia, M. T.; Trubetskoy, V.; Torchilin, V.; Langer, R. *Science* **1994**, *263*, 1600.
(10) Scholz, G.; Iijima, M.; Nagasaki, Y.; Kataoka, K. *Macromolecules* **1995**, *28*, 7295.
(11) Wilczek-Vera, G.; Danis, P. O.; Eisenberg, A. *Macromolecules* **1996**, *29*, 4036.
(12) Wilczek-Vera, G.; Yu, Y.; Waddell, K.; Danis, P. O.; Eisenberg, A. *Macromelecules* **1999**, *32*, 2180.
(13) Belenkii, B. G.; Gankina, E. S.; Tennikov, M. B.; Vilenchik, L. Z. *J. Chromatogr.* **1978**, *147*, 99.
(14) Entelis, S. G.; Evreinov, V. V.; Gorshkov, A. V. *Adv. Polym. Sci.* **1986**, *76*, 129.
(15) Guttman, C. M.; DiMarzio, E. A.; Douglas, J. F. *Macromolecules* **1996,** *29*, 5723.
(16) Falkenhagen, J.; Much, H.; Stauf, W.; Müller, A. H. E. *Macromolecules* **2000**, *33*, 3687.
(17) Lee, H.; Lee, W.; Chang, T.; Choi, S.; Lee, D.; Ji, H.; Nonidez, W. K.; Mays, J. W. *Macromolecules* **1999**, *32*, 4143.
(18) Xu, Y.; Teraoka, I. *Macromolecules* **1998**, *31*, 4143.
(19) Zheng, H.; Teraoka, I. *Macromol. Chem. Phys.* **2001**, *202*, 765.
(20) Zheng, H.; Teraoka, I., submitted to *Macromolecules*.
(21) Fujiwara, T.; Kimura, Y.; Teraoka, I. *J. Polym. Sci., Polym. Chem. Ed.* **2000**, *38*, 2405.
(22) Fujiwara, T.; Kimura, Y.; Teraoka, I. *Polymer* **2001**, *42*, 1067.
(23) Lee, C. W.; Kimura, Y. *Bull. Chem. Soc. Jpn.* **1996**, *69*, 1787.
(24) Fujiwara, T.; Miyamoto, M.; Kimura, Y. *Macromolecules* **2000**, *33*, 2782.
(25) Dube, A.; Teraoka, I. *Macromelecules* **1997**, *30*, 7753.
(26) Zhuravlev, L. T. *Langmuir* **1987**, *3*, 316.
(27) Jeon, S. H.; Ree, T. *J. Polym. Sci., Polym. Chem. Ed.* **1988**, *26*, 1419.
(28) Maunu, S. L.; Kinnunen, J.; Soljamo, K.; Sundholm, F. *Polymer* **1993**, *34*, 1141.
(29) Plueddemann, E. P. *Silane Coupling Agents*; Plenum Press: New York, 1991.

MA0101207